Fermilab-Pub-08/457-E

Evidence of $WW + WZ$ production with lepton + jets final states in $p\bar{p}$ collisions at $\sqrt{s} = 1.96$ TeV

V.M. Abazov[36], B. Abbott[75], M. Abolins[65], B.S. Acharya[29], M. Adams[51], T. Adams[49], E. Aguilo[6], M. Ahsan[59], G.D. Alexeev[36], G. Alkhazov[40], A. Alton[64,a], G. Alverson[63], G.A. Alves[2], M. Anastasoaie[35], L.S. Ancu[35], T. Andeen[53], B. Andrieu[17], M.S. Anzelc[53], M. Aoki[50], Y. Arnoud[14], M. Arov[60], M. Arthaud[18], A. Askew[49,b], B. Åsman[41], A.C.S. Assis Jesus[3], O. Atramentov[49], C. Avila[8], F. Badaud[13], L. Bagby[50], B. Baldin[50], D.V. Bandurin[59], P. Banerjee[29], S. Banerjee[29], E. Barberis[63], A.-F. Barfuss[15], P. Bargassa[80], P. Baringer[58], J. Barreto[2], J.F. Bartlett[50], U. Bassler[18], D. Bauer[43], S. Beale[6], A. Bean[58], M. Begalli[3], M. Begel[73], C. Belanger-Champagne[41], L. Bellantoni[50], A. Bellavance[50], J.A. Benitez[65], S.B. Beri[27], G. Bernardi[17], R. Bernhard[23], I. Bertram[42], M. Besançon[18], R. Beuselinck[43], V.A. Bezzubov[39], P.C. Bhat[50], V. Bhatnagar[27], G. Blazey[52], F. Blekman[43], S. Blessing[49], K. Bloom[67], A. Boehnlein[50], D. Boline[62], T.A. Bolton[59], E.E. Boos[38], G. Borissov[42], T. Bose[77], A. Brandt[78], R. Brock[65], G. Brooijmans[70], A. Bross[50], D. Brown[81], X.B. Bu[7], N.J. Buchanan[49], D. Buchholz[53], M. Buehler[81], V. Buescher[22], V. Bunichev[38], S. Burdin[42,c], T.H. Burnett[82], C.P. Buszello[43], P. Calfayan[25], S. Calvet[16], J. Cammin[71], M.A. Carrasco-Lizarraga[33], E. Carrera[49], W. Carvalho[3], B.C.K. Casey[50], H. Castilla-Valdez[33], S. Chakrabarti[72], D. Chakraborty[52], K.M. Chan[55], A. Chandra[48], E. Cheu[45], D.K. Cho[62], S. Choi[32], B. Choudhary[28], L. Christofek[77], T. Christoudias[43], S. Cihangir[50], D. Claes[67], J. Clutter[58], M. Cooke[50], W.E. Cooper[50], M. Corcoran[80], F. Couderc[18], M.-C. Cousinou[15], S. Crépé-Renaudin[14], V. Cuplov[59], D. Cutts[77], M. Ćwiok[30], H. da Motta[2], A. Das[45], G. Davies[43], K. De[78], S.J. de Jong[35], E. De La Cruz-Burelo[33], C. De Oliveira Martins[3], K. DeVaughan[67], F. Déliot[18], M. Demarteau[50], R. Demina[71], D. Denisov[50], S.P. Denisov[39], S. Desai[50], H.T. Diehl[50], M. Diesburg[50], A. Dominguez[67], T. Dorland[82], A. Dubey[28], L.V. Dudko[38], L. Duflot[16], S.R. Dugad[29], D. Duggan[49], A. Duperrin[15], S. Dutt[27], J. Dyer[65], A. Dyshkant[52], M. Eads[67], D. Edmunds[65], J. Ellison[48], V.D. Elvira[50], Y. Enari[77], S. Eno[61], P. Ermolov[38,‡], H. Evans[54], A. Evdokimov[73], V.N. Evdokimov[39], A.V. Ferapontov[59], T. Ferbel[61,71], F. Fiedler[24], F. Filthaut[35], W. Fisher[50], H.E. Fisk[50], M. Fortner[52], H. Fox[42], S. Fu[50], S. Fuess[50], T. Gadfort[70], C.F. Galea[35], C. Garcia[71], A. Garcia-Bellido[71], V. Gavrilov[37], P. Gay[13], W. Geist[19], W. Geng[15,65], C.E. Gerber[51], Y. Gershtein[49,b], D. Gillberg[6], G. Ginther[71], B. Gómez[8], A. Goussiou[82], P.D. Grannis[72], H. Greenlee[50], Z.D. Greenwood[60], E.M. Gregores[4], G. Grenier[20], Ph. Gris[13], J.-F. Grivaz[16], A. Grohsjean[25], S. Grünendahl[50], M.W. Grünewald[30], F. Guo[72], J. Guo[72], G. Gutierrez[50], P. Gutierrez[75], A. Haas[70], N.J. Hadley[61], P. Haefner[25], S. Hagopian[49], J. Haley[68], I. Hall[65], R.E. Hall[47], L. Han[7], K. Harder[44], A. Harel[71], J.M. Hauptman[57], J. Hays[43], T. Hebbeker[21], D. Hedin[52], J.G. Hegeman[34], A.P. Heinson[48], U. Heintz[62], C. Hensel[22,d], K. Herner[72], G. Hesketh[63], M.D. Hildreth[55], R. Hirosky[81], T. Hoang[49], J.D. Hobbs[72], B. Hoeneisen[12], M. Hohlfeld[22], S. Hossain[75], P. Houben[34], Y. Hu[72], Z. Hubacek[10], V. Hynek[9], I. Iashvili[69], R. Illingworth[50], A.S. Ito[50], S. Jabeen[62], M. Jaffré[16], S. Jain[75], K. Jakobs[23], C. Jarvis[61], R. Jesik[43], K. Johns[45], C. Johnson[70], M. Johnson[50], D. Johnston[67], A. Jonckheere[50], P. Jonsson[43], A. Juste[50], E. Kajfasz[15], D. Karmanov[38], P.A. Kasper[50], I. Katsanos[70], V. Kaushik[78], R. Kehoe[79], S. Kermiche[15], N. Khalatyan[50], A. Khanov[76], A. Kharchilava[69], Y.N. Kharzheev[36], D. Khatidze[70], T.J. Kim[31], M.H. Kirby[53], M. Kirsch[21], B. Klima[50], J.M. Kohli[27], J.-P. Konrath[23], A.V. Kozelov[39], J. Kraus[65], T. Kuhl[24], A. Kumar[69], A. Kupco[11], T. Kurča[20], V.A. Kuzmin[38], J. Kvita[9], F. Lacroix[13], D. Lam[55], S. Lammers[70], G. Landsberg[77], P. Lebrun[20], W.M. Lee[50], A. Leflat[38], J. Lellouch[17], J. Li[78,‡], L. Li[48], Q.Z. Li[50], S.M. Lietti[5], J.K. Lim[31], J.G.R. Lima[52], D. Lincoln[50], J. Linnemann[65], V.V. Lipaev[39], R. Lipton[50], Y. Liu[7], Z. Liu[6], A. Lobodenko[40], M. Lokajicek[11], P. Love[42], H.J. Lubatti[82], R. Luna-Garcia[33,e], A.L. Lyon[50], A.K.A. Maciel[2], D. Mackin[80], R.J. Madaras[46], P. Mättig[26], A. Magerkurth[64], P.K. Mal[82], H.B. Malbouisson[3], S. Malik[67], V.L. Malyshev[36], Y. Maravin[59], B. Martin[14], R. McCarthy[72], M.M. Meijer[35], A. Melnitchouk[66], L. Mendoza[8], P.G. Mercadante[5], M. Merkin[38], K.W. Merritt[50], A. Meyer[21], J. Meyer[22,d], J. Mitrevski[70], R.K. Mommsen[44], N.K. Mondal[29], R.W. Moore[6], T. Moulik[58], G.S. Muanza[15], M. Mulhearn[70], O. Mundal[22], L. Mundim[3], E. Nagy[15], M. Naimuddin[50], M. Narain[77], H.A. Neal[64], J.P. Negret[8], P. Neustroev[40], H. Nilsen[23], H. Nogima[3], S.F. Novaes[5], T. Nunnemann[25], D.C. O'Neil[6], G. Obrant[40], C. Ochando[16], D. Onoprienko[59], N. Oshima[50], N. Osman[43], J. Osta[55], R. Otec[10], G.J. Otero y Garzón[50], M. Owen[44], P. Padley[80], M. Pangilinan[77], N. Parashar[56], S.-J. Park[22,d], S.K. Park[31], J. Parsons[70], R. Partridge[77], N. Parua[54], A. Patwa[73], G. Pawloski[80], B. Penning[23], M. Perfilov[38], K. Peters[44], Y. Peters[26], P. Pétroff[16], M. Petteni[43], R. Piegaia[1], J. Piper[65], M.-A. Pleier[22], P.L.M. Podesta-Lerma[33,f], V.M. Podstavkov[50],

Y. Pogorelov[55], M.-E. Pol[2], P. Polozov[37], B.G. Pope[65], A.V. Popov[39], C. Potter[6], W.L. Prado da Silva[3], H.B. Prosper[49], S. Protopopescu[73], J. Qian[64], A. Quadt[22,d], B. Quinn[66], A. Rakitine[42], M.S. Rangel[2], K. Ranjan[28], P.N. Ratoff[42], P. Renkel[79], P. Rich[44], M. Rijssenbeek[72], I. Ripp-Baudot[19], F. Rizatdinova[76], S. Robinson[43], R.F. Rodrigues[3], M. Rominsky[75], C. Royon[18], P. Rubinov[50], R. Ruchti[55], G. Safronov[37], G. Sajot[14], A. Sánchez-Hernández[33], M.P. Sanders[17], B. Sanghi[50], G. Savage[50], L. Sawyer[60], T. Scanlon[43], D. Schaile[25], R.D. Schamberger[72], Y. Scheglov[40], H. Schellman[53], T. Schliephake[26], S. Schlobohm[82], C. Schwanenberger[44], A. Schwartzman[68], R. Schwienhorst[65], J. Sekaric[49], H. Severini[75], E. Shabalina[51], M. Shamim[59], V. Shary[18], A.A. Shchukin[39], R.K. Shivpuri[28], V. Siccardi[19], V. Simak[10], V. Sirotenko[50], P. Skubic[75], P. Slattery[71], D. Smirnov[55], G.R. Snow[67], J. Snow[74], S. Snyder[73], S. Söldner-Rembold[44], L. Sonnenschein[17], A. Sopczak[42], M. Sosebee[78], K. Soustruznik[9], B. Spurlock[78], J. Stark[14], V. Stolin[37], D.A. Stoyanova[39], J. Strandberg[64], S. Strandberg[41], M.A. Strang[69], E. Strauss[72], M. Strauss[75], R. Ströhmer[25], D. Strom[53], L. Stutte[50], S. Sumowidagdo[49], P. Svoisky[35], A. Sznajder[3], A. Tanasijczuk[1], W. Taylor[6], B. Tiller[25], F. Tissandier[13], M. Titov[18], V.V. Tokmenin[36], I. Torchiani[23], D. Tsybychev[72], B. Tuchming[18], C. Tully[68], P.M. Tuts[70], R. Unalan[65], L. Uvarov[40], S. Uvarov[40], S. Uzunyan[52], B. Vachon[6], P.J. van den Berg[34], R. Van Kooten[54], W.M. van Leeuwen[34], N. Varelas[51], E.W. Varnes[45], I.A. Vasilyev[39], P. Verdier[20], L.S. Vertogradov[36], M. Verzocchi[50], D. Vilanova[18], F. Villeneuve-Seguier[43], P. Vint[43], P. Vokac[10], M. Voutilainen[67,g], R. Wagner[68], H.D. Wahl[49], M.H.L.S. Wang[50], J. Warchol[55], G. Watts[82], M. Wayne[55], G. Weber[24], M. Weber[50,h], L. Welty-Rieger[54], A. Wenger[23,i], N. Wermes[22], M. Wetstein[61], A. White[78], D. Wicke[26], M.R.J. Williams[42], G.W. Wilson[58], S.J. Wimpenny[48], M. Wobisch[60], D.R. Wood[63], T.R. Wyatt[44], Y. Xie[77], C. Xu[64], S. Yacoob[53], R. Yamada[50], W.-C. Yang[44], T. Yasuda[50], Y.A. Yatsunenko[36], H. Yin[7], K. Yip[73], H.D. Yoo[77], S.W. Youn[53], J. Yu[78], C. Zeitnitz[26], S. Zelitch[81], T. Zhao[82], B. Zhou[64], J. Zhu[72], M. Zielinski[71], D. Zieminska[54], A. Zieminski[54,‡], L. Zivkovic[70], V. Zutshi[52], and E.G. Zverev[38]

(The DØ Collaboration)

[1]*Universidad de Buenos Aires, Buenos Aires, Argentina*
[2]*LAFEX, Centro Brasileiro de Pesquisas Físicas, Rio de Janeiro, Brazil*
[3]*Universidade do Estado do Rio de Janeiro, Rio de Janeiro, Brazil*
[4]*Universidade Federal do ABC, Santo André, Brazil*
[5]*Instituto de Física Teórica, Universidade Estadual Paulista, São Paulo, Brazil*
[6]*University of Alberta, Edmonton, Alberta, Canada, Simon Fraser University, Burnaby, British Columbia, Canada, York University, Toronto, Ontario, Canada, and McGill University, Montreal, Quebec, Canada*
[7]*University of Science and Technology of China, Hefei, People's Republic of China*
[8]*Universidad de los Andes, Bogotá, Colombia*
[9]*Center for Particle Physics, Charles University, Prague, Czech Republic*
[10]*Czech Technical University, Prague, Czech Republic*
[11]*Center for Particle Physics, Institute of Physics, Academy of Sciences of the Czech Republic, Prague, Czech Republic*
[12]*Universidad San Francisco de Quito, Quito, Ecuador*
[13]*LPC, Université Blaise Pascal, CNRS/IN2P3, Clermont, France*
[14]*LPSC, Université Joseph Fourier Grenoble 1, CNRS/IN2P3, Institut National Polytechnique de Grenoble, Grenoble, France*
[15]*CPPM, Aix-Marseille Université, CNRS/IN2P3, Marseille, France*
[16]*LAL, Université Paris-Sud, IN2P3/CNRS, Orsay, France*
[17]*LPNHE, IN2P3/CNRS, Universités Paris VI and VII, Paris, France*
[18]*CEA, Irfu, SPP, Saclay, France*
[19]*IPHC, Université Louis Pasteur, CNRS/IN2P3, Strasbourg, France*
[20]*IPNL, Université Lyon 1, CNRS/IN2P3, Villeurbanne, France and Université de Lyon, Lyon, France*
[21]*III. Physikalisches Institut A, RWTH Aachen University, Aachen, Germany*
[22]*Physikalisches Institut, Universität Bonn, Bonn, Germany*
[23]*Physikalisches Institut, Universität Freiburg, Freiburg, Germany*
[24]*Institut für Physik, Universität Mainz, Mainz, Germany*
[25]*Ludwig-Maximilians-Universität München, München, Germany*
[26]*Fachbereich Physik, University of Wuppertal, Wuppertal, Germany*
[27]*Panjab University, Chandigarh, India*
[28]*Delhi University, Delhi, India*
[29]*Tata Institute of Fundamental Research, Mumbai, India*
[30]*University College Dublin, Dublin, Ireland*

[31]Korea Detector Laboratory, Korea University, Seoul, Korea
[32]SungKyunKwan University, Suwon, Korea
[33]CINVESTAV, Mexico City, Mexico
[34]FOM-Institute NIKHEF and University of Amsterdam/NIKHEF, Amsterdam, The Netherlands
[35]Radboud University Nijmegen/NIKHEF, Nijmegen, The Netherlands
[36]Joint Institute for Nuclear Research, Dubna, Russia
[37]Institute for Theoretical and Experimental Physics, Moscow, Russia
[38]Moscow State University, Moscow, Russia
[39]Institute for High Energy Physics, Protvino, Russia
[40]Petersburg Nuclear Physics Institute, St. Petersburg, Russia
[41]Lund University, Lund, Sweden, Royal Institute of Technology and Stockholm University, Stockholm, Sweden, and Uppsala University, Uppsala, Sweden
[42]Lancaster University, Lancaster, United Kingdom
[43]Imperial College, London, United Kingdom
[44]University of Manchester, Manchester, United Kingdom
[45]University of Arizona, Tucson, Arizona 85721, USA
[46]Lawrence Berkeley National Laboratory and University of California, Berkeley, California 94720, USA
[47]California State University, Fresno, California 93740, USA
[48]University of California, Riverside, California 92521, USA
[49]Florida State University, Tallahassee, Florida 32306, USA
[50]Fermi National Accelerator Laboratory, Batavia, Illinois 60510, USA
[51]University of Illinois at Chicago, Chicago, Illinois 60607, USA
[52]Northern Illinois University, DeKalb, Illinois 60115, USA
[53]Northwestern University, Evanston, Illinois 60208, USA
[54]Indiana University, Bloomington, Indiana 47405, USA
[55]University of Notre Dame, Notre Dame, Indiana 46556, USA
[56]Purdue University Calumet, Hammond, Indiana 46323, USA
[57]Iowa State University, Ames, Iowa 50011, USA
[58]University of Kansas, Lawrence, Kansas 66045, USA
[59]Kansas State University, Manhattan, Kansas 66506, USA
[60]Louisiana Tech University, Ruston, Louisiana 71272, USA
[61]University of Maryland, College Park, Maryland 20742, USA
[62]Boston University, Boston, Massachusetts 02215, USA
[63]Northeastern University, Boston, Massachusetts 02115, USA
[64]University of Michigan, Ann Arbor, Michigan 48109, USA
[65]Michigan State University, East Lansing, Michigan 48824, USA
[66]University of Mississippi, University, Mississippi 38677, USA
[67]University of Nebraska, Lincoln, Nebraska 68588, USA
[68]Princeton University, Princeton, New Jersey 08544, USA
[69]State University of New York, Buffalo, New York 14260, USA
[70]Columbia University, New York, New York 10027, USA
[71]University of Rochester, Rochester, New York 14627, USA
[72]State University of New York, Stony Brook, New York 11794, USA
[73]Brookhaven National Laboratory, Upton, New York 11973, USA
[74]Langston University, Langston, Oklahoma 73050, USA
[75]University of Oklahoma, Norman, Oklahoma 73019, USA
[76]Oklahoma State University, Stillwater, Oklahoma 74078, USA
[77]Brown University, Providence, Rhode Island 02912, USA
[78]University of Texas, Arlington, Texas 76019, USA
[79]Southern Methodist University, Dallas, Texas 75275, USA
[80]Rice University, Houston, Texas 77005, USA
[81]University of Virginia, Charlottesville, Virginia 22901, USA and
[82]University of Washington, Seattle, Washington 98195, USA

(Dated: October 21, 2008)

We present the first evidence of $WW+WZ$ production with lepton+jets final states at a hadron collider. The data correspond to 1.07 fb^{-1} of integrated luminosity collected with the D0 detector at the Fermilab Tevatron Collider in $p\bar{p}$ collisions at $\sqrt{s}=1.96$ TeV. The observed cross section for $WW+WZ$ production is 20.2 ± 4.5 pb, consistent with the SM prediction of 16.1 ± 0.9 pb. The probability for background fluctuations to produce an excess equal to or larger than that observed is estimated to be $5.4{\times}10^{-6}$, corresponding to a significance of 4.4 standard deviations.

PACS numbers: 14.70.Fm, 14.70.Hp, 13.85.Ni, 13.85.Qk

The production of weak vector boson pairs (WW, WZ, or ZZ) in $p\bar{p}$ collisions at the Fermilab Tevatron Collider has so far been observed only in fully leptonic final states [1, 2]. These processes provide tests of the electroweak sector of the standard model (SM) through the measurement of self-interactions of the vector bosons. Deviations from SM predictions for the production rates or kinematic distributions of the bosons or their decay products could indicate the presence of new physics. Final states containing two weak bosons are also relevant to searches for the Higgs boson or for new particles in extensions of the SM.

In this Letter we report the first evidence at a hadron collider for the production of a W boson decaying leptonically associated with a second vector boson V (V=W or Z) that decays hadronically ($WV\to \ell\nu q\bar{q}$; ℓ=e,μ). The limited dijet mass resolution results in a significant overlap of the $W\to q\bar{q}$ and $Z\to q\bar{q}$ dijet mass peaks; therefore, WW and WZ are considered simultaneously, assuming the the ratio of their cross sections as predicted by the SM. Previous searches for WV production in lepton+jets final states [3, 4] were hindered by the large background from the production of jets in association with a W boson (W+jets). The use of improved multivariate event classification and new statistical techniques [5], as well as an increased integrated luminosity, make the WV signal in lepton+jets final states more distinguishable from the W+jets background and more accessible to measurement. This analysis provides a proving ground for these advanced techniques now ubiquitous in Higgs searches at the Tevatron.

We analyze 1.07 fb^{-1} of data collected with the D0 detector [6] at a center-of-mass energy of 1.96 TeV at the Tevatron. Candidates for $e\nu q\bar{q}$ must pass a trigger with a single electron or electron+jet(s) requirement, giving an efficiency of 98^{+2}_{-3}%. A suite of triggers for $\mu\nu q\bar{q}$ candidates achieves an efficiency of 100^{+0}_{-5}%.

To select $WV\to \ell\nu q\bar{q}$ candidate events, we require: a single reconstructed lepton (electron or muon) [7] with transverse momentum $p_T > 20$ GeV and pseudorapidity $|\eta| < 1.1$ (2.0) for electrons (muons); the imbalance in transverse energy to be $\not\!\!E_T > 20$ GeV; and at least two jets [8] with $p_T > 20$ GeV and $|\eta| < 2.5$. The highest p_T jet must satisfy $p_T > 30$ GeV. To reduce background from processes that do not contain $W\to \ell\nu$, we require a "transverse" W mass [9] of $M_T^W > 35$ GeV. The lepton must be spatially match to a track reconstructed in the central tracking system and originating from the primary vertex. Electrons (muons) must be isolated from other particles in the calorimeter (and central tracking system).

Signal and background processes containing a charged lepton are modeled via Monte Carlo (MC) simulation. The diboson signal (WW and WZ) events are generated with PYTHIA [10] using CTEQ6L parton distribution functions (PDFs). The fixed-order matrix element (FOME) generator ALPGEN [11] with CTEQ6L1 PDFs is used to generate W+jets, Z+jets, and $t\bar{t}$ events to leading order at the parton level. The FOME generator COMPHEP [12] is used to produce single top quark MC samples. ALPGEN and COMPHEP are interfaced to PYTHIA for subsequent parton showering and hadronization. All simulated events undergo a GEANT-based [13] detector simulation and are reconstructed using the same programs as D0 data. Samples are normalized using next-to-leading-order (NLO) or next-to-next-to-leading-order predictions for SM cross sections, except W+jets, which is scaled to the data.

The probability for multijet events with misidentified leptons to pass all selection requirements is small; however, because of the copious production of multijet events, the background from this source cannot be ignored. For $\mu\nu q\bar{q}$, the multijet background is modeled with data that fail the muon isolation requirements, but pass all other selections. The normalization is determined from a fit to the M_T^W distribution. For $e\nu q\bar{q}$, the multijet background is estimated using a "loose-but-not-tight" data sample obtained by selecting events that pass loosened electron quality requirements, but fail the tight electron quality criteria [7]. This sample is normalized by the probability for a jet that passes the "loose" electron requirements to also pass the tight requirement. Both $\mu\nu q\bar{q}$ and $e\nu q\bar{q}$ multijet samples are corrected for the contributions from processes we model through MC.

Accurate modeling of the selected events is vital. The dominant background contribution is W+jets; thus the modeling of the ALPGEN W+jets sample and sources of uncertainty are studied in detail. Comparison of ALPGEN with other generators and with data shows discrepancies [14] in jet η and dijet angular separation. The data are therefore used to correct these quantities in the ALPGEN W+jets and Z+jets MC samples. The possible bias to this procedure from the presence of diboson signal in the data is small, but nevertheless taken into account via a systematic uncertainty. Systematic effects on the differential distributions of the ALPGEN W+jets and Z+jets MC samples due to variations of the renormalization and factorization scales and of the parameters used in the MLM parton-jet matching algorithm [15] are also considered. Uncertainties on PDFs, as well as uncertainties from object reconstruction and identification, are evaluated for all MC samples. We consider the effect of systematic uncertainty both on the normalization and on the shape of differential distributions for signal and backgrounds [16].

The signal and the backgrounds are further separated using a multivariate classifier to combine information from several kinematic variables. This analysis uses a Random Forest (RF) classifier [17]. When supplied with a set of events for training the RF creates an ensemble of decision tree classifiers [17], each designed to differentiate signal from background. The RF evaluates events by averaging the outputs from all of the trees. Thirteen

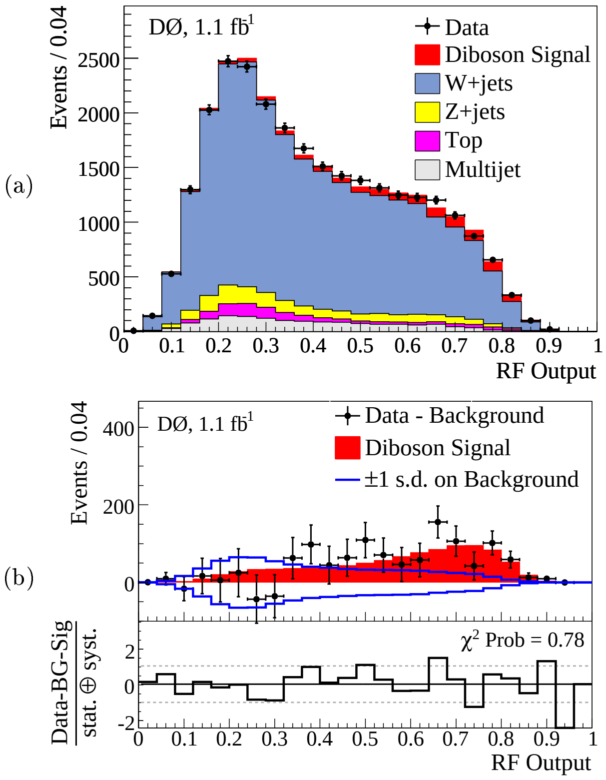

FIG. 1: (a) The RF output distribution from the combined $e\nu q\bar{q}$ and $\mu\nu q\bar{q}$ channels for data and MC predictions following the fit of MC to data. (b) A comparison of the signal (filled histograms) to background-subtracted data (points) in the same distribution. Also shown is the ±1 standard deviation (s.d.) systematic uncertainty on the background prediction and the residual distance from the signal for each point divided by the total uncertainty.

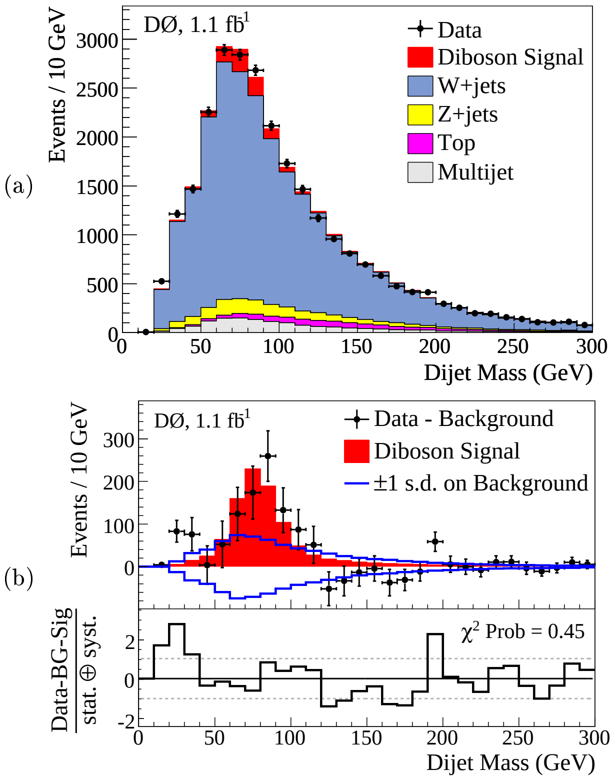

FIG. 2: (a) The dijet mass distribution from the combined $e\nu q\bar{q}$ and $\mu\nu q\bar{q}$ channels for data and MC predictions after the combined fit of the RF output. (b) A comparison of the signal (filled histograms) to background-subtracted data (points) in the same distribution. Also shown is the ±1 standard deviation (s.d.) systematic uncertainty on the background prediction and the residual distance from the signal for each point divided by the total uncertainty.

TABLE I: Measured number of events for signal and each background after the combined fit (with total uncertainties as determined from the fit) and the observed number of data events.

	$e\nu q\bar{q}$ channel	$\mu\nu q\bar{q}$ channel
Diboson signal	436 ± 36	527 ± 43
W+jets	10100 ± 500	11910 ± 590
Z+jets	387 ± 61	1180 ± 180
$t\bar{t}$ + single top	436 ± 57	426 ± 54
Multijet	1100 ± 200	328 ± 83
Total predicted	12460 ± 550	14370 ± 620
Data	12473	14392

well-modeled kinematic variables [16] that demonstrate a difference in probability density between signal and at least one of the backgrounds, such as dijet mass and $\not{E}_T$, are used as inputs to the RF. The RF is trained using half of each MC sample. The other halves, along with the multijet background samples, are then evaluated by the RF to be used for the measurement.

The signal cross section is determined from a fit of signal and background RF templates to the data by minimizing a Poisson χ^2 function with respect to variations in the systematic uncertainties [5]. A Gaussian prior is used for each systematic uncertainty. Different uncertainties are assumed to be mutually independent, but those common to multiple samples or lepton channels are assumed to be 100% correlated.

The fit simultaneously varies the WV and W+jets contributions, thereby also determining the normalization factor for the W+jets MC sample. This obviates the need for using the predicted ALPGEN cross section, and provides a more rigorous approach that incorporates an unbiased uncertainty from W+jets when extracting the WV cross section. The normalization factor yielded by the fit for the W+jets ALPGEN prediction is 1.53 ± 0.13, similar to the expected ratio of NLO to LO cross sections [18]. The measured yields for signal and each background are given in Table I. Table II contains the measured WV cross section for the each channel separately and combined, showing consistent results between the channels and with the SM prediction

TABLE II: The signal cross section extracted from a simultaneous fit of the WV cross section and the normalization factor for W+jets. Also given are the expected and observed p-values obtained by comparing the measurement with pseudo-experiments assuming no signal, along with the corresponding significance in number of standard deviations (s.d.) for the corresponding one-sided Gaussian integral.

Channel	Fitted signal σ (pb)	Expected p-value (significance)	Observed p-value (significance)
$e\nu q\bar{q}$ RF Output	18.0±3.7(stat)±5.2(sys)±1.1(lum)	6.8×10^{-3} (2.5 s.d.)	3.2×10^{-3} (2.7 s.d.)
$\mu\nu q\bar{q}$ RF Output	22.8±3.3(stat)±4.9(sys)±1.4(lum)	1.8×10^{-3} (2.9 s.d.)	5.2×10^{-5} (3.9 s.d.)
Combined RF Output	20.2±2.5(stat)±3.6(sys)±1.2(lum)	1.5×10^{-4} (3.6 s.d.)	5.4×10^{-6} (4.4 s.d.)
Combined Dijet Mass	18.5±2.8(stat)±4.9(sys)±1.1(lum)	1.7×10^{-3} (2.9 s.d.)	4.4×10^{-4} (3.3 s.d.)

of $\sigma(WV) = 16.1 \pm 0.9$ pb [19]. The combined fit yields a cross section of 20.2 ± 2.5(stat) $\pm$ 3.6(sys) $\pm$ 1.2(lum) pb. The combined RF output distributions following the combined fit are shown in Fig. 1 along with a comparison between the background-subtracted data and the signal. Figure 2 shows analogous plots for the dijet mass after the combined fit of the RF output. The dominant systematic uncertainties arise from the modeling of the W+jets background and the jet energy scale [16]. The position of the dijet mass peaks in data and MC are consistent within one half standard deviation, including the relative data/MC energy scale uncertainty. As a cross check, we also perform the measurement using only the dijet mass distribution. The result, also given in Table II, is consistent with the result obtained using the RF output, though less precise.

The significance of the measurement is obtained via fits of the signal+background hypothesis to pseudo-data samples drawn from the background-only hypothesis [20]. The observed (expected) significance corresponds to the fraction of outcomes that yield a WV cross section at least as large as that measured in data (predicted by the SM). The probabilities that background fluctuations could produce the expected and observed signal in each channel, separately and combined, are shown in Table II along with the corresponding significance (number of standard deviations corresponding to the equivalent one-sided Gaussian probability).

In summary, we measure $\sigma(WV) = 20.2 \pm 4.5$ pb (with V=W or Z) in $p\bar{p}$ collisions at $\sqrt{s} = 1.96$ TeV. This result is consistent with the SM value of $\sigma(WV) = 16.1 \pm 0.9$ pb [19]. The probability that the backgrounds fluctuate to give an excess equal to or larger than the excess observed in data is 5.4×10^{-6}, corresponding to a significance of 4.4 standard deviations. This represents the first evidence for WV production in lepton+jets events at a hadron collider and is consistent with previous measurements of WW and WZ yields in fully leptonic final states [1, 2]. This work further provides a validation of the analytical methods used in searches for Higgs bosons at the Tevatron [21].

We thank the staffs at Fermilab and collaborating institutions, and acknowledge support from the DOE and NSF (USA); CEA and CNRS/IN2P3 (France); FASI, Rosatom and RFBR (Russia); CNPq, FAPERJ, FAPESP and FUNDUNESP (Brazil); DAE and DST (India); Colciencias (Colombia); CONACyT (Mexico); KRF and KOSEF (Korea); CONICET and UBACyT (Argentina); FOM (The Netherlands); STFC (United Kingdom); MSMT and GACR (Czech Republic); CRC Program, CFI, NSERC and WestGrid Project (Canada); BMBF and DFG (Germany); SFI (Ireland); The Swedish Research Council (Sweden); CAS and CNSF (China); and the Alexander von Humboldt Foundation (Germany).

[a] Visitor from Augustana College, Sioux Falls, SD, USA.
[b] Visitor from Rutgers University, Piscataway, NJ, USA.
[c] Visitor from The University of Liverpool, Liverpool, UK.
[d] Visitor from II. Physikalisches Institut, Georg-August-University, Göttingen, Germany.
[e] Visitor from Centro de Investigacion en Computacion - IPN, Mexico City, Mexico.
[f] Visitor from ECFM, Universidad Autonoma de Sinaloa, Culiacán, Mexico.
[g] Visitor from Helsinki Institute of Physics, Helsinki, Finland.
[h] Visitor from Universität Bern, Bern, Switzerland.
[i] Visitor from Universität Zürich, Zürich, Switzerland.
[‡] Deceased.

[1] D0 Collaboration: V. M. Abazov *et al.*, Phys. Rev. Lett. **94**, 151801 (2005); Phys. Rev. D **76**, 111104(R) (2007); arXiv:0808.0703 [hep-ex] (2008).
[2] CDF Collaboration: D. Acosta *et al.*, Phys. Rev. Lett. **94**, 211801 (2005); A. Abulencia *et al.*, Phys. Rev. Lett. **98**, 161801 (2007); T. Aaltonen *et al.*, Phys. Rev. Lett. **100**, 201801 (2008).
[3] B. Abbott *et al.* (D0 Collaboration), Phys. Rev. D **62**, 052005 (2000).
[4] T. Aaltonen *et al.* (CDF Collaboration), Phys. Rev. D **76**, 111103(R) (2007).
[5] W. Fisher, FERMILAB-TM-2386-E (2006).
[6] B. Abbott *et al.* (D0 Collaboration), Nucl. Instrum. Methods Phys. Res. A **565**, 463 (2006).
[7] V. M. Abazov *et al.* (D0 Collaboration), Phys. Lett. B **626**, 45 (2005).
[8] G. C. Blazey *et al.*, arXiv:hep-ex/0005012 (2000). The seeded cone algorithm with radius 0.5 was used.
[9] J. Smith, W. L. van Neerven, and J. A. M. Vermaseren,

Phys. Rev. Lett. **50**, 1738 (1983).
[10] T. Sjöstrand *et al.*, Comput. Phys. Commun. **135**, 238 (2001). Verison 6.3 was used.
[11] M. L. Mangano *et al.*, JHEP **0307**, 001 (2003). Version 2.05 was used.
[12] A. Pukhov *et al.*, arXiv:hep-ph/9908288 (2000).
[13] R. Brun, F. Carminati, CERN Program Library Long Writeup W5013 (1993).
[14] J. Alwall *et al.*, Eur. Phys. C **53**, 473 (2008).
[15] S. Höche *et al.*, arXiv:hep-ph/0602031 (2006).
[16] See attached supplemental material.
[17] I. Narsky, arXiv:physics/0507143 [physics.data-an] (2005).
[18] J. M. Campbell and R. K. Ellis, Phys. Rev. D **65**, 113007 (2002).
[19] J. M. Campbell and R. K. Ellis, Phys. Rev. D **60**, 113006 (1999). Cross sections were calculated with the same parameters given in the paper, except with $\sqrt{s} = 1.96$ TeV.
[20] V. M. Abazov *et al.* (D0 Collaboration), Phys. Rev. D **78**, 012005 (2008).
[21] TEVNPH Working Group, for the CDF Collaboration and D0 Collaboration, arXiv:0804.3423 [hep-ex] (2008).

SUPPLEMENTAL MATERIAL

Systematic Uncertainties

Table III gives the systematic uncertainties in percent for Monte Carlo simulations and multijet estimates. We consider the effect of systematic uncertainty both on the normalization and on the shape of differential distributions for signal and backgrounds. Though Table III lists an uncertainty for the W+jets simulation, this uncertainty is not used when measuring the diboson signal cross section, for which the W+jets normalization is a free parameter. However, the size of the uncertainty must be specified for generating the pseudodata used in the significance estimation. Also given in the table is the contribution of each systematic uncertainty to the total systematic uncertainty of 3.6 pb on the measured cross section, $\sigma^{\rm meas}(WV)$. This total systematic unceratinty is obtained from the systematic uncertainties on the parameter of the fit to the RF output, $\sigma^{\rm meas}(WV)/\sigma^{\rm th}(WV)$, multiplying them with the theoretical cross section $\sigma^{\rm th}(WV)$. Therefore, the additional uncertainty on the integrated luminosity of the data sample (6.1%) is considered separately.

Random Forest Input Variables

The 13 kinematic variables used in the Random Forest classifier are listed below. The variables are derived from characteristics of objects reconstructed from observables in each event and can be loosely classified into three categories: variables based on the kinematics of individual objects, variables based on the kinematics of multiple objects, and variables based on the angular relationships of objects. Several variables are calculated using the four-momentum of the dijet system or the leptonic W boson candidate ($W^{\rm lept}$). The dijet system is defined as the four-momentum sum of the highest p_T jet (jet$_1$) and second highest p_T jet (jet$_2$). $W^{\rm lept}$ is reconstructed from the charged lepton and the $\not\!\!E_T$. The neutrino from the $W\to \ell\nu$ decay is assigned the transverse momentum from the $\not\!\!E_T$ and a longitudinal momentum calculated from the quadratic condition satisfying $M_W = 80.3$ GeV. Of the two possible solutions, we choose the one that minimizes the total event invariant mass.

- **Kinematics of Individual Objects:**
  1. The imbalance in transverse energy ($\not\!\!E_T$), which is the imbalance in transverse momentum as determined by summing the energies of calorimeter cells and corrected for the transverse momenta of muons and the energy scale corrections for jets and electrons in the event.
  2. The second highest jet p_T: $p_T(\text{jet}_2)$.
- **Kinematics of Multiple Objects:**
  1. The "transverse W mass" reconstructed from the charged lepton and the $\not\!\!E_T$: $M_T(W) = \sqrt{2\, p_T^\ell\, \not\!\!E_T\, (1-\cos(\Delta\phi(\ell,\not\!\!E_T)))}$.
  2. The p_T of the $W^{\rm lept}$ candidate.
  3. The invariant mass of the dijet system.
  4. The magnitude of the leading jet momentum perpendicular to the dijet system: $\frac{|\vec{p}_T(\text{jet}_1+\text{jet}_2)\times\vec{p}_T(\text{jet}_1)|}{|\vec{p}_T(\text{jet}_1+\text{jet}_2)|}$, where "$\times$" represents the cross product relation. This variable is calculated in the rest frame of the $W^{\rm lept}$ candidate.
  5. The magnitude of the second-leading jet momentum perpendicular to the dijet system: $\frac{|\vec{p}_T(\text{jet}_1+\text{jet}_2)\times\vec{p}_T(\text{jet}_2)|}{|\vec{p}_T(\text{jet}_1+\text{jet}_2)|}$, where "$\times$" represents the cross product relation. This variable is calculated in the laboratory frame.
  6. The angular separation between the two highest p_T jets, weighted by the relative transverse momentum of the second-leading jet and the $W^{\rm lept}$ candidate: $\Delta R(\text{jet}_1,\text{jet}_2)\frac{p_T(\text{jet}_2)}{p_T(\ell)+\not\!\!E_T}$. This variable is calculated in the rest frame of the $W^{\rm lept}$ candidate.
  7. The "centrality" of the charged lepton and jets system, given by the scalar sum of transverse momenta divided by the sum of energy for the charged lepton and all jets in the event.
- **Angular Relationships of Objects:**
  1. The azimuthal separation between the charged lepton and the $\not\!\!E_T$: $\Delta\phi(\ell,\not\!\!E_T)$.
  2. The cosine of the angle between the dijet system and the leading jet in the laboratory frame: $\cos(\angle(\text{jet}_1,\text{dijet}))$.
  3. The cosine of the angle between the dijet system and the second-leading jet in the laboratory frame: $\cos(\angle(\text{jet}_2,\text{dijet}))$.
  4. Cosine of the angle between leading jet and the $W^{\rm lept}$ candidate: $\cos(\angle(\text{jet}_1,W^{\rm lept}))$, evaluated in the rest frame of the dijet system.

TABLE III: Systematic uncertainties in percent for Monte Carlo simulations and multijet estimates. Uncertainties are identical for both lepton channels except where otherwise indicated. The nature of the uncertainty, *i.e.*, whether it refers to a differential dependence (D) or just normalization (N), is also provided. The values for uncertainties with a differential dependence correspond to the maximum amplitude of the fluctuations in the RF output. Also provided is the contribution of each source to the total systematic uncertainty of 3.6 pb on the measured cross section, which does not include the additional uncertainty of 6.1% due to the luminosity.

Source of systematic uncertainty	Diboson signal	W+jets	Z+jets	Top	Multijet	Nature	$\Delta\sigma$ (pb)
Trigger efficiency, $e\nu q\bar{q}$ channel	$+2/-3$	$+2/-3$	$+2/-3$	$+2/-3$		N	< 0.1
Trigger efficiency, $\mu\nu q\bar{q}$ channel	$+0/-5$	$+0/-5$	$+0/-5$	$+0/-5$		D	< 0.1
Lepton identification	± 4	± 4	± 4	± 4		N	< 0.1
Jet identification	± 1	± 1	± 1	$\pm <1$		D	0.3
Jet energy scale	± 4	± 9	± 9	± 4		D	1.9
Jet energy resolution	± 3	± 4	± 4	± 4		N	< 0.1
Cross section		± 20[a]	± 6	± 10		N	1.1
Multijet normalization, $e\nu q\bar{q}$ channel					± 20	N	0.9
Multijet normalization, $\mu\nu q\bar{q}$ channel					± 30	N	0.5
Multijet shape, $e\nu q\bar{q}$ channel					± 6	D	< 0.1
Multijet shape, $\mu\nu q\bar{q}$ channel					± 10	D	< 0.1
Diboson signal NLO/LO shape	± 10					D	< 0.1
Parton distribution function	± 1	± 1	± 1	± 1		D	0.2
ALPGEN η and ΔR corrections		± 1	± 1			D	< 0.1
Renormalization and factorization scale		± 3	± 3			D	0.9
ALPGEN parton-jet matching parameters		± 4	± 4			D	2.4

[a] The cross section uncertainty on W+jets is not used when measuring the diboson signal cross section (the W+jets normalization is a free parameter); however, it is necessary for generating pseudo-data used in the significance estimation.